
# Surface profiling of cellulose, hemicellulose, and lignin in softwood Kraft handsheets by reference-guided ToF-SIMS

Carbohydrate Polymer Technologies and Applications 15 (2026) 101209

Contents lists available at ScienceDirect

Carbohydrate Polymer Technologies and Applications

journal homepage: www.sciencedirect.com/journal/carbohydrate-polymer-technologies-and-applications

# Surface profiling of cellulose, hemicellulose, and lignin in softwood Kraft handsheets by reference-guided ToF-SIMS

Nivedhitha Venkatraman [a,b], Per A. Larsson [b,c], Anette Larsson [a,b,d], Per Malmberg [a,b,*]

[a] Department of Chemistry and Chemical Engineering, Chalmers University of Technology, Gothenburg, Sweden
[b] FibRe Centre for Lignocellulose-based Thermoplastics, Chalmers University of Technology, Gothenburg, Sweden
[c] Department of Fibre and Polymer Technology, KTH, Stockholm, Sweden
[d] Wallenberg Wood Science Center, Chalmers University of Technology, Gothenburg, Sweden

ARTICLE INFO

*Keywords:*
Cellulose
Chemometrics
Hemicellulose
Softwood Kraft handsheets
Surface profiling
ToF-SIMS

ABSTRACT

The surface composition of softwood Kraft fiber materials, particularly the relative contributions of cellulose, hemicelluloses, and lignin at fiber surfaces, strongly influences interfacial properties relevant to paper performance and surface modification. Because these properties are governed by the outermost fiber surface rather than by bulk composition alone, methods capable of resolving chemically heterogeneous lignocellulosic surfaces are needed. Time-of-flight secondary ion mass spectrometry (ToF-SIMS) is attractive for this purpose because it provides surface-sensitive and chemically resolved information, but its spectra are complicated by fragment overlap, adduct formation, matrix effects, and contamination. Here, a semi-quantitative ToF-SIMS workflow was developed using compacted reference samples, total-ion-count normalization, pairwise principal component analysis, and conservative marker-ion validation. Unbleached and bleached handsheets were used to assess whether the workflow could detect bleaching-induced chemical differences at softwood Kraft fiber surfaces. The analysis reproducibly differentiated lignin- and polysaccharide-associated ion patterns. Unbleached handsheets showed higher relative contributions from guaiacyl lignin-associated fragments, whereas bleached handsheets showed enhanced polysaccharide-associated signals. Two-dimensional chemical imaging supported these trends by visualizing the spatial distribution of assigned marker ions across the handsheet surfaces. The workflow provides a practical, semi-quantitative surface-characterization method for pulp fibers surfaces, fiber modification, adhesive and coating interfaces, and related bio-based material surfaces.

## 1. Introduction

Softwood Kraft fiber materials are multicomponent carbohydrate-rich systems in which the relative surface exposure of cellulose, hemicelluloses, and lignin changes during pulping and strongly affects interfacial behavior. During pulping and bleaching, chemically heterogeneous fiber surfaces are produced, and their local composition influences inter-fiber bonding, wettability, mechanical performance and chemical reactivity (Åvitsland et al., 2005; Eliasson et al., 2023; Forsström et al., 2005; Henrik-Klemens et al., 2024; Henriksson et al., 2024; Jin et al., 2022; Koljonen et al., 2004a; Wålinder et al., 2001). However, conventional bulk chemical analyses do not resolve surface-specific variations in such complex lignocellulosic fibers. This limitation has motivated the use of surface-sensitive techniques such as ESCA/XPS, ATR-FTIR, Raman spectroscopy, AFM and SEM to examine pulp fiber surface chemistry, morphology and processing-induced changes (Fardim et al., 2003; Fardim & Holmbom, 2005; Laine et al., 1994, 1996). XPS provides elemental and carbon-bonding information, while ATR-FTIR and Raman spectroscopy provide functional-group fingerprints of carbohydrate- and lignin-associated structures (Agarwal et al., 1997; Kesari et al., 2020; Paulsson et al., 2003; Risén et al., 2004). AFM and SEM provide surface-morphological and topographical context (Fardim et al., 2003; Fardim & Holmbom, 2005; Kleen et al., 2002). However, these methods do not provide the same fragment-level ion specificity or ion-specific chemical imaging as Time-of-flight secondary ion mass spectrometry (ToF-SIMS) (Mou et al., 2016; Watts et al., 2021). On the other hand, conventional ToF-SIMS technique requires ultra-high vacuum and therefore characterizes dehydrated rather than

* Corresponding author at: Department of Chemistry and Chemical Engineering, Chalmers University of Technology, Gothenburg, Sweden.
*E-mail address:* per.malmberg@chalmers.se (P. Malmberg).

https://doi.org/10.1016/j.carpta.2026.101209

Available online 27 July 2026

fully hydrated fibre surfaces.

ToF-SIMS is well-suited for surface analysis of carbohydrate-rich fiber materials because it provides label-free molecular fragment information with nanometer-scale surface sensitivity and high lateral resolution (Vickerman, 2013). With its ability to operate in both spectroscopic and imaging modes, ToF-SIMS can provide both characteristic fragment ions and visualize their spatial distributions, supporting the differentiation of cellulose-, hemicellulose-, and lignin-associated chemistries at fiber surfaces (Letourneau et al., 2023; Mou et al., 2016; Tokareva et al., 2011; Tolbert et al., 2016). Early ToF-SIMS studies primarily focused on elucidating lignin-derived fragment chemistry using isolated lignin, synthetic model compounds, and chemically modified systems, thereby establishing characteristic ions associated with guaiacyl and syringyl units (Kleen, 2005; Reale et al., 2004; Saito et al., 2006, 2005). These foundational investigations provided essential insight into lignin fragmentation pathways and enabled subsequent application of ToF-SIMS to more complex lignocellulosic materials. Subsequent studies extended ToF-SIMS to intact wood, pulp, and fiber systems, where lignin and polysaccharides coexist at heterogeneous surfaces, and showed that the technique can detect processing-induced changes in the relative abundances of lignin- and polysaccharide-associated ions (Braham et al., 2015; Fardim et al., 2003; Fardim & Holmbom, 2005; Koljonen, 2004; Lucia, 2001).

Goacher et al. (2011) demonstrated the capability of high-resolution ToF-SIMS to map lignin- and polysaccharide-associated chemistry in intact wood. Later work addressed practical considerations for ToF-SIMS analysis of lignocellulosic substrates, including the influence of enzymatic treatments and exposure to aqueous pH-controlled salt solutions on wood surface spectra (Goacher et al., 2018, 2013), as well as the identification and mitigation of salt-induced spectral interferences that can mask characteristic ions (Braham et al., 2015). Zhou et al. (2011) demonstrated that ToF-SIMS could directly resolve and spatially differentiate guaiacyl and syringyl lignin in poplar wood, revealing their distinct localization patterns across vessel and fiber cell walls. Notably, the authors systematically evaluated ToF-SIMS ion markers for lignin and polysaccharides using reference compounds and wood cell wall sections, providing a framework for assigning spectral features to specific lignocellulosic components. Despite these advances, subsequent studies have emphasized the challenge posed by isobaric fragment overlap and the need for careful marker selection supported by multivariate analysis, spatial mapping, and consistency with established chemical trends (Watts et al., 2021). While these studies established ToF-SIMS as a sensitive technique for probing lignocellulosic surface chemistry, practical and reproducible data-analysis workflows for heterogeneous fiber surfaces remain limited. In particular, marker-ion assignment for polysaccharide-associated signals, supported by smooth reference surfaces and systematic pairwise multivariate analysis, remains limited. To address this gap, the present study develops a semi-quantitative ToF-SIMS workflow for chemically complex softwood Kraft handsheet surfaces, in which marker-ion assignment is guided by compacted reference samples. Total-ion-count (TIC) normalized spectra were interpreted semi-quantitatively to compare relative ion patterns across reference samples and handsheet surfaces, thereby mitigating differences in overall secondary-ion yield (Lee et al., 2008). The TIC-normalized datasets were then interpreted semi-quantitatively using relative ion intensities, and spatial distributions where relevant, to differentiate polysaccharide- and lignin-associated surface features.

The primary aim was to establish a practical workflow for distinguishing polysaccharide- and lignin-associated ion patterns at chemically heterogeneous softwood Kraft handsheet surfaces. Such surfaces are characterized by overlapping fragment-ion signals, pronounced surface heterogeneity, adduct formation and contamination, all of which can hinder confident spectral interpretation. Softwood Kraft handsheets prepared from bleached and unbleached fibers were selected to validate the workflow, as bleaching is expected to alter the relative balance between lignin-associated and polysaccharide-associated surface signals, thereby providing a chemically meaningful contrast. The methodology integrates: (i) preparation of flat, uniform reference surfaces by mechanically compacting powdered microcrystalline cellulose, galactoglucomannan, xylan, and residual lignin to minimize topography-related background effects and improve the reproducibility of reference spectra used for marker-ion assignment; (ii) systematic pairwise principal component analysis (PCA) comparisons between handsheets and reference samples to obtain chemically interpretable separation; and (iii) conservative peak-assignment criteria that explicitly screen for common contaminants and salt-derived adducts. We hypothesize that ToF-SIMS, when applied with compacted reference samples to gain smoother surfaces, total-ion-count normalization and systematic chemometric analysis, can reproducibly distinguish lignin-, polysaccharide-associated ion patterns at chemically heterogeneous softwood Kraft handsheet surfaces, despite substantial overlaps in fragment chemistry.

## 2. Materials and methods

### 2.1. Materials and sample preparation

Microcrystalline cellulose (MCC) powder was sourced from Sigma-Aldrich (cat. 435,236), with a nominal particle size of 51 μm, pH 6.3 for an 11 wt% slurry, and a bulk density of 0.6 g $mL^{-1}$ at 25 °C. Beechwood xylan (Sigma-Aldrich, X4252; CAS 9014–63–5) was used as received; supplier specification ≥90% xylan, supplied as powder. Galactoglucomannan (GGM) was a kind gift from Stora Enso AB (Karlstad, Sweden) and produced as described in Oinonen (2014). Briefly, the GGM was recovered from the process-water stream of a thermomechanical pulping line, concentrated by membrane filtration, and subsequently precipitated using ethanol. GGM reference contained 62.0 wt.% polysaccharides, 0.5 wt.% lignin, and 2.3 wt.% ash. The polysaccharide fraction was composed of mannose (50%), xylose (17%), glucose (13%), arabinose (10%), and galactose (10%), as previously reported. The monosaccharide composition (galactose: glucose: mannose) was approximately 0.8:1:4.1. The powder was stored at room temperature in sealed containers, and no additional drying was performed prior to compaction. The residual lignin, hereafter referred to as softwood Kraft pulp lignin (SKPL), was a kind gift from Åke Henrik-Klemens and was isolated from unbleached, never-dried softwood Kraft pulp by enzymatic hydrolysis of carbohydrates followed by mild acidolysis in dioxane/water, as described by Henrik-Klemens et al. (2024) using a protocol adapted from Guerra et al. (2007); Jääskeläinen et al. (2003). This lignin sample also contained: ash 0.8 wt.%, residual carbohydrate 0.9 wt.%, and protein 4.7 wt.% (from CHN nitrogen with factor 8×N), corresponding to a calculated lignin purity of 93.6 wt.%.

MCC was used as a cellulose-rich reference representing a glucose-dominated carbohydrate surface, whereas GGM and xylan were selected as hemicellulose reference samples, where GGM provided a hexose-rich hemicellulose reference, while xylan provided a pentose-rich hemicellulose reference. SKPL was included as the lignin-rich reference to support discrimination between polysaccharide- and lignin-associated secondary ions during the marker-ion screening. The reference materials were selected as chemically enriched component models to support conservative marker-ion assignment rather than to reproduce the complete chemical composition and supramolecular organization of native softwood fiber surfaces.

MCC, GGM, xylan, and SKPL powders were compacted using ellipse manual tablet press, model HA 03 - 451 TO 101 02, and a die with a diameter of ~12 mm, to produce flat reference surfaces, thereby reducing topography-dependent differences in secondary-ion extraction and eliminating background contributions from the double-sided mounting tape.

Never-dried unbleached and bleached softwood Kraft pulps (USK and BSK, respectively) (Stora Enso, Skoghall, Karlstad, Sweden, with a mix of spruce and pine fibers) were characterized prior to handsheet

formation. Handsheets were prepared using a Rapid Köthen sheet former (ISO 5269–2:2004; TAPPI/ANSI T 205 sp-18), and complete chemical characterization is given in Table 1.

### 2.2. Time-of-Flight secondary ion mass spectrometry

Mass spectrometry was conducted using a ToF-SIMS 5 instrument (ION-TOF GmbH, Münster, Germany) equipped with a 30 keV $Bi^{3+}$ cluster ion source. Depending on the measurement requirements, the instrument was operated in spectroscopy or imaging mode, under the ultra-high vacuum conditions ($E^{-7}$-$E^{-9}$ mbar). In spectroscopy mode, the $Bi^{3+}$ beam was focused on a nominal spot size of approximately 1 μm. Spectra were acquired over a 100 × 100 μm area with a primary ion current of 0.55 pA, a cycle time of 125 μs, and a total of 20 scans per measurement. For each handsheet, six independent surface locations distributed across a single representative sheet were analysed under identical instrumental conditions. These independent measurement positions were used for all multivariate analyses to capture within-sheet surface heterogeneity. Charge compensation was applied using the instrument's electron flood gun during analysis of the insulating to minimize local surface charging, thereby improving mass accuracy and the reproducibility of secondary-ion emission. All samples were analysed under charge-compensation and identical instrumental conditions, and spectra were subsequently TIC-normalized to minimize systematic variability between measurements samples. This produced a mass resolution of m/Δm ≥ 2000 at full width at half maximum (FWHM) at *m/z* 200 for the USK handsheet and ≥ 1700 for the BSK handsheet. The mass resolution of the compacted reference samples (MCC, GGM, and SKPL) was ≥ 6000. As the compacted reference samples yielded higher mass resolution than the handsheets, the reference spectra were used primarily for marker-ion screening and assignment support, whereas inter-sample comparisons were performed using a common peak list and identical mass-interval binning across all spectra. For 2D imaging, measurements were performed over a 500 × 500 $\mu m^2$ area using a random raster pattern with a pixel resolution of 256 × 256 pixels to visualize the spatial distribution of the marker ions across representative fiber-network regions. A total of 25 scans were acquired per image using a primary ion current of 0.41 pA. A photograph of the mounted samples in the ToF-SIMS back mount, including the compacted powder samples and handsheets, is shown in Figure S1.

### 2.3. Data processing and multivariate analysis

Data acquisition and evaluation of images and mass spectral data were conducted using the SurfaceLab software (version 7.4, ION-TOF). Mass calibration was performed separately for lignin- and polysaccharide-rich samples to ensure accurate mass assignment across the spectral range, particularly in the low-mass region. For polysaccharide-rich samples, calibration was based on characteristic low-mass carbohydrate fragments such as $C_2H_3^+$, $C_3H_5^+$, $C_2H_5O^+$, and $C_6H_{12}O_5^+$. For lignin-rich samples, calibration was based on low-mass aromatic and benzylic fragment ions such as $C_6H_5^+$, $C_8H_9^+$, $C_9H_7^+$, and $C_9H_{11}O_3^+$ (Goacher et al., 2011). A peak list was generated from all the samples, and each peak was defined with a mass interval tolerance of ±0.03 u. Additionally, the narrow binning improved isobaric resolution, enabling differentiation between chemically distinct ions with nearly identical nominal masses. This interval list was applied across all spectra to enable consistent comparison between samples. Spectra and the 2D images were normalized to TIC to reduce differences in overall secondary-ion yield and improve comparability across replicate measurements and sample classes. The integrated peak areas at all masses were then exported to a spreadsheet. An unsupervised multivariate analysis method was employed to discern chemical patterns in complex spectral datasets. The compacted reference samples were used to support marker-ion screening and to anchor pairwise comparisons with the handsheets. PCA was performed in OriginPro, version 2023 (OriginLab Corporation, Northampton, MA, USA), using the Principal Component Analysis for Spectroscopy application, v1.42. Only peaks with a signal-to-noise ratio of at least 10 were retained for further analysis. Replicate spectra were acquired from six independent surface locations per sample class and treated as independent observations for univariate statistical analysis.

**Table 1**
Chemical characterization of USK and BSK pulps used for handsheet preparation.

| Property* | BSK | USK | Method/standard |
|---|---|---|---|
| Total lignin content (wt.%) | 1.1 | 13.0 | TAPPI UM 250 |
| Klason lignin (wt.%) | 0.5 | 12.4 | TAPPI UM 250 |
| Acid-soluble lignin (wt.%) | 0.6 | 0.6 | TAPPI UM 250 |
| Arabinose (anhydro) (mg $g^{-1}$) | 6 | 11 | Monosaccharide analysis |
| Galactose (anhydro) (mg $g^{-1}$) | 2 | 8 | Monosaccharide analysis |
| Glucose (anhydro) (mg $g^{-1}$) | 868 | 681 | Monosaccharide analysis |
| Xylose (anhydro) (mg $g^{-1}$) | 72 | 81 | Monosaccharide analysis |
| Mannose (anhydro) (mg $g^{-1}$) | 65 | 56 | Monosaccharide analysis |
| Ash content at 925 °C (%) | 0.30 | 0.85 | ISO 1762 |
| $Na^+$ (μmol $g^{-1}$) | 41.7 | 100.0 | ICP-OES |
| Ca (μmol $g^{-1}$) | 3.7 | 27.4 | ICP-OES |
| Fe (μmol $g^{-1}$) | 0.08 | 0.20 | ICP-OES |

The full analytical characterizations of GGM, SKPL, and the handsheets are summarized in Supplementary Information Table ST1–3.

## 3. Results and discussion

To develop a ToF-SIMS workflow for lignocellulosic materials, powdered reference samples with different particle-size distributions (MCC, SKPL, xylan and GGM) were compacted using flat punches. This preparation produced flatter and more reproducible reference surfaces, thereby reducing background contributions and sample-to-sample matrix variability compared with loose powder smears. The improved surface quality increased the mass resolution (m/Δm) from ≥1700 in the powder smears to ≥6000 at *m/z* 200 after compaction, strengthening confidence in subsequent marker-ion selection and assignment. The resulting compacted references were then used to support the interpretation of chemically heterogeneous handsheet surfaces.

### 3.1. Assigned marker-ion library for carbohydrate-polymer surfaces

The handsheets presented rough, topographically non-uniform fiber-network surfaces compared to the compacted reference samples. The reduced variation in the surface topography led to more consistent ion extraction and improved spectral stability, making the compacted MCC, GGM, xylan, and SKPL samples suitable for marker-ion screening. Fig. 1a–f show surface micrographs of compacted MCC, GGM, SKPL, and xylan, together with the USK and BSK handsheets. The comparison of mass resolution at *m/z* equal to $163^+$ for different sample types (handsheets, powder adhered to tape, and compacted powder reference) is shown in Figure S2.

Fig. 2a shows representative fragment spectra from the compacted reference samples, whereas Fig. 2b shows the corresponding spectra from USK and BSK handsheets. Compared with the compacted reference samples, the handsheet spectra showed less distinct fragment patterns. This is attributed to the more complex surface of the handsheets, where surface roughness, local chemical heterogeneity, and fiber–fiber overlaps can contribute to variable secondary-ion yields and overlapping fragment signals. Therefore, the handsheet spectra cannot be interpreted by direct visual comparison with the reference spectra alone. Instead, marker-ion assignment was supported by replicate measurements and chemometric analysis, allowing chemically meaningful trends to be distinguished from topography- and matrix-related variability. Representative spectra for all individual samples are shown in Figure S3.

Because the handsheet spectra contained overlapping contributions from cellulose, hemicellulose, and lignin, direct visual comparison with

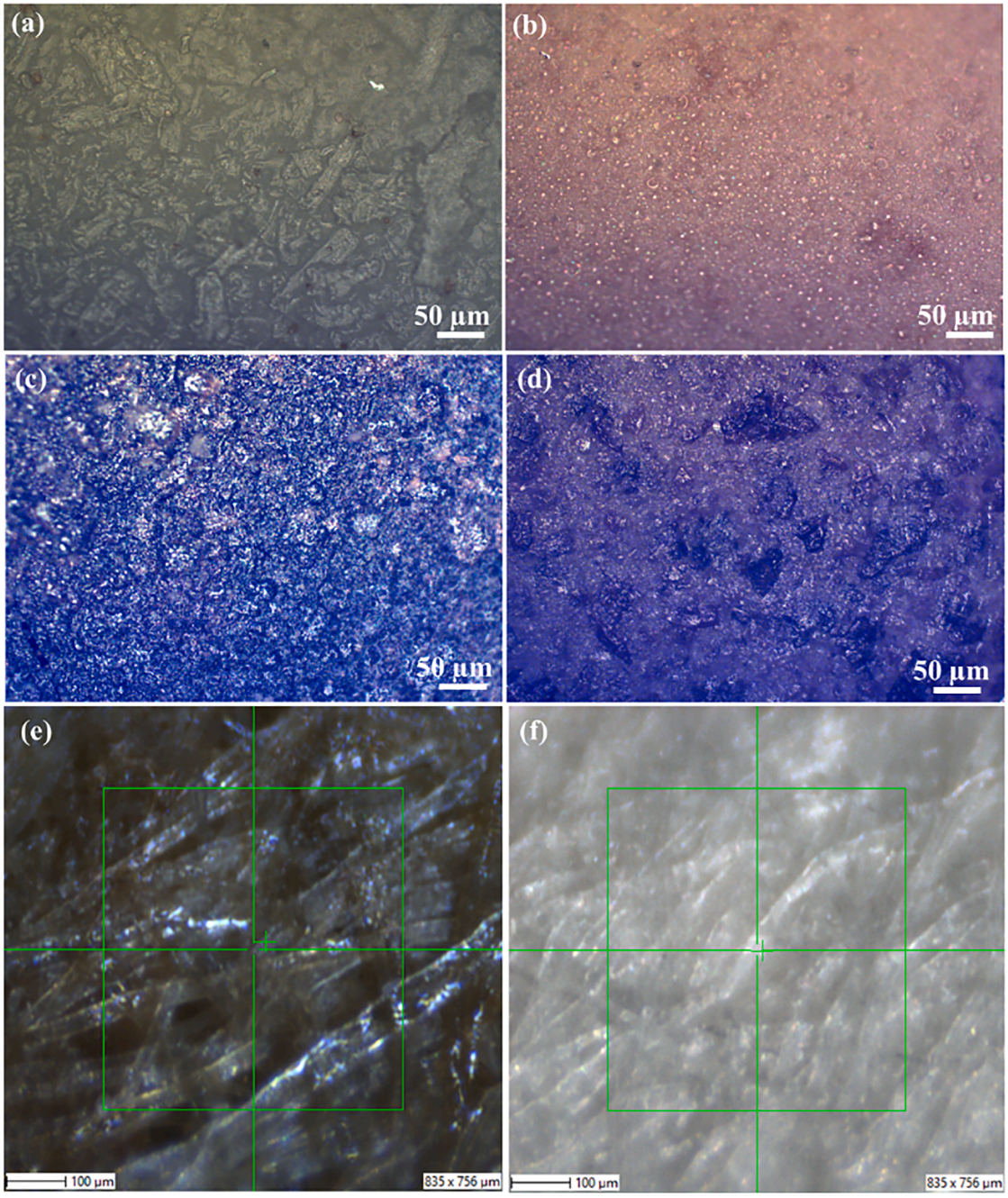


**Fig. 1.** Optical micrographs of the surfaces analyzed by ToF-SIMS: compacted reference samples of (a) MCC, (b) GGM, (c) SKPL, and (d) xylan, and handsheet surfaces of (e) USK and (f) BSK. In panels (e, f), the green overlay indicates the selected ToF-SIMS analysis area and instrument positioning crosshair.

the reference spectra was insufficient for reliable marker-ion assignment. Therefore, a series of pairwise PCA models was constructed to simplify the chemical contrasts and improve interpretability (Table 2). The reference-sample comparisons were first used to identify ions associated with defined lignocellulosic components by polysaccharide, and lignin-rich SKPL samples. These assignments were then used to support the interpretation of the USK and BSK handsheet spectra. Marker ions were retained only when they were detected consistently across the six replicate spectra within a sample class, contributed to the relevant PCA loadings, and remained chemically plausible after considering common contaminants and salt-derived adducts, as discussed in Section 3.2. No replicate spectra were excluded as outliers. This conservative workflow allowed polysaccharide- and lignin-associated ion signals to be distinguished more confidently in the chemically heterogeneous handsheet surfaces.

Fig. 3a shows a clear separation between USK and BSK handsheets in the PCA score plot. The tight clustering of replicate measurements and the separation along PC1, which captures 78% of the total variance, indicate reproducible differences in surface composition between the USK and BSK handsheet surfaces. The corresponding loading plot is shown in Fig. 3b. For chemical interpretability, the loading plot is displayed only up to $m/z$ 400. In contrast, higher-mass ions were dominated mainly by extractives- and fatty-acid-related fragments, which were not the primary focus in this study and could obscure the interpretation of the carbohydrate- and lignin-associated fragments. The remaining pairwise PCA score and loading plots (PCA2–8) are shown in Figures S4–S10.

In Fig. 3b, USK handsheet spectra, located on the positive side of

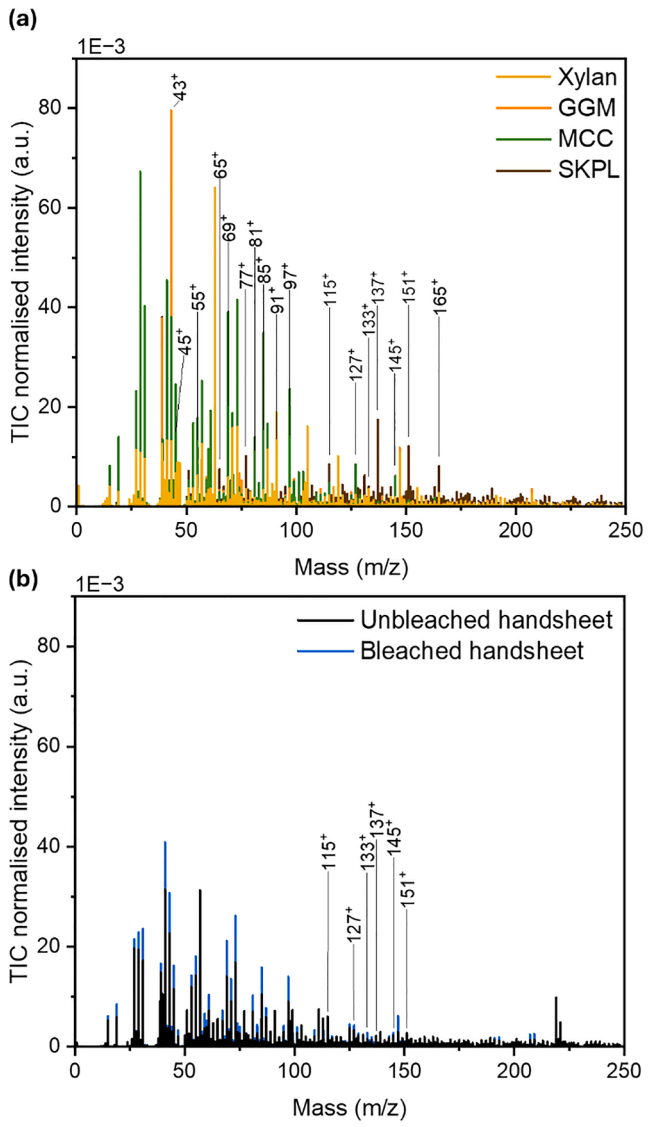


**Fig. 2.** Representative positive-ion ToF-SIMS spectra from (a) compacted reference samples of xylan, GGM, MCC and SKPL, and (b) USK and BSK handsheet surfaces.

PC1, were associated with ions consistent with residual softwood lignin. This is chemically reasonable because USK pulp retains a higher contribution from guaiacyl-rich lignin than BSK. The main lignin-associated ions were *m/z* 137.1 ($C_8H_9O_2^+$) and *m/z* 151.0 ($C_8H_7O_3^+$), which are widely reported as guaiacyl-type fragments in softwood materials (Fardim et al., 2003; Goacher et al., 2011; Saito et al., 2005; Tokareva et al., 2011), with *m/z* 137.1$^+$ commonly assigned to a protonated guaiacol-type ion. Additional oxygenated lignin-related ions at *m/z* 167.1 ($C_9H_{11}O_3^+$) and *m/z* 181.1 ($C_9H_9O_4^+$) also contributed to the positive PC1 loading and are commonly associated with S-type lignin fragments (Goacher et al., 2011; Morreel et al., 2010; Saito et al., 2006; Zhou et al., 2011).

In contrast, the BSK fiber handsheet, positioned on the negative side of PC1, was associated mainly with polysaccharides-related ions, including *m/z* 85.0 ($C_4H_5O_2^+$), 97.0 ($C_5H_5O_2^+$), 115.0 ($C_5H_7O_3^+$), 127.0 ($C_6H_7O_3^+$), 133.0 ($C_5H_9O_4^+$), and 145.0 ($C_6H_9O_4^+$). Within this group, *m/z* 127$^+$,145$^+$, and 133$^+$ are consistent with hexose-derived fragments associated with polysaccharide-rich surfaces (Goacher et al., 2011; Tokareva et al., 2011). The loading pattern in Fig. 3b therefore supports a bleaching-related decrease in the relative contribution of lignin-associated surface chemistry. The agreement between these marker-ion trends and previously reported lignin- and polysaccharide-associated assignments supports the use of this reference-guided workflow for interpreting chemically complex Kraft fiber surfaces (Fardim et al., 2003; Fardim & Holmbom, 2005; Goacher et al., 2011; Saito et al., 2006).

The present workflow adopts a conservative, multi-criterion strategy for marker-ion selection rather than relying solely on PCA loading magnitude. Marker ion candidates were required to (i) contribute meaningfully to class separation in the PCA loading plots, (ii) agree with the reference-guided assignments obtained from the compacted cellulose-, hemicellulose-, and lignin-rich reference materials, (iii) be consistently assigned in previous ToF-SIMS studies, and (iv) exhibit sufficient chemical specificity to permit confident assignment to the lignocellulosic component of interest. Consequently, ions with conflicting literature assignments or insufficient chemical specificity were excluded from the final marker-ion set despite contributing to the PCA separation. Accordingly, the ion at *m/z* 115$^+$ was not included in the final marker-ion set despite its association with the BSK surface. Previous ToF-SIMS studies have assigned this nominal mass to both lignin-derived and xylan-associated fragments (Fardim et al., 2003; Goacher et al., 2011; Mou et al., 2016; Zhou et al., 2011). Consequently, in softwood Kraft fiber surfaces containing both lignin and

**Table 2**
Pairwise PCA models used to support chemical interpretation of ToF-SIMS data.

| PCA model | Sample comparison | Main separation | Chemical interpretation from PCA separation |
|---|---|---|---|
| PCA1 | USK vs BSK handsheets | Bleaching-related contrast in relative lignin-associated and polysaccharide-associated surface signals | Used to assess whether bleaching altered the relative contributions of lignin-associated and polysaccharide-associated ions at handsheet surfaces. |
| PCA2 | MCC vs SKPL | Polysaccharides-associated vs lignin-associated fragment patterns | Used to assess the contrast between cellulose-associated and lignin-associated fragment ions using a simplified reference sample. |
| PCA3 | MCC vs GGM | Cellulose vs softwood hemicellulose | Used to examine GGM-associated fragment ions relative to the dominant glucose-derived fragments of cellulose. |
| PCA4 | MCC vs xylan | Cellulose vs xylan-rich hemicellulose | Used to examine fragment ions associated with pentose-rich xylan relative to cellulose. |
| PCA5 | USK handsheet vs SKPL | USK handsheet surface vs lignin-rich reference with shared lignin-associated contributions | Used to assess which polysaccharide-associated fragment ions remain distinguishable in the USK handsheet despite the presence of residual lignin shared with SKPL. |
| PCA6 | BSK handsheet vs MCC | BSK handsheet surface vs polysaccharides-rich reference | Used to assess which non-cellulosic fragment ions remain distinguishable at the BSK handsheet surface relative to cellulose. |
| PCA7 | BSK handsheet vs GGM | BSK handsheet surface vs polysaccharides-rich hemicellulose reference | Used to examine hemicellulose-associated fragment ions within the BSK handsheet surface. |
| PCA8 | USK handsheet vs GGM | USK handsheet surface vs polysaccharides-rich hemicellulose reference under lignin-containing conditions | Used to examine which hemicellulose-associated fragment ions remain detectable when GGM-related signals are embedded within the lignin-containing USK handsheet surface. |

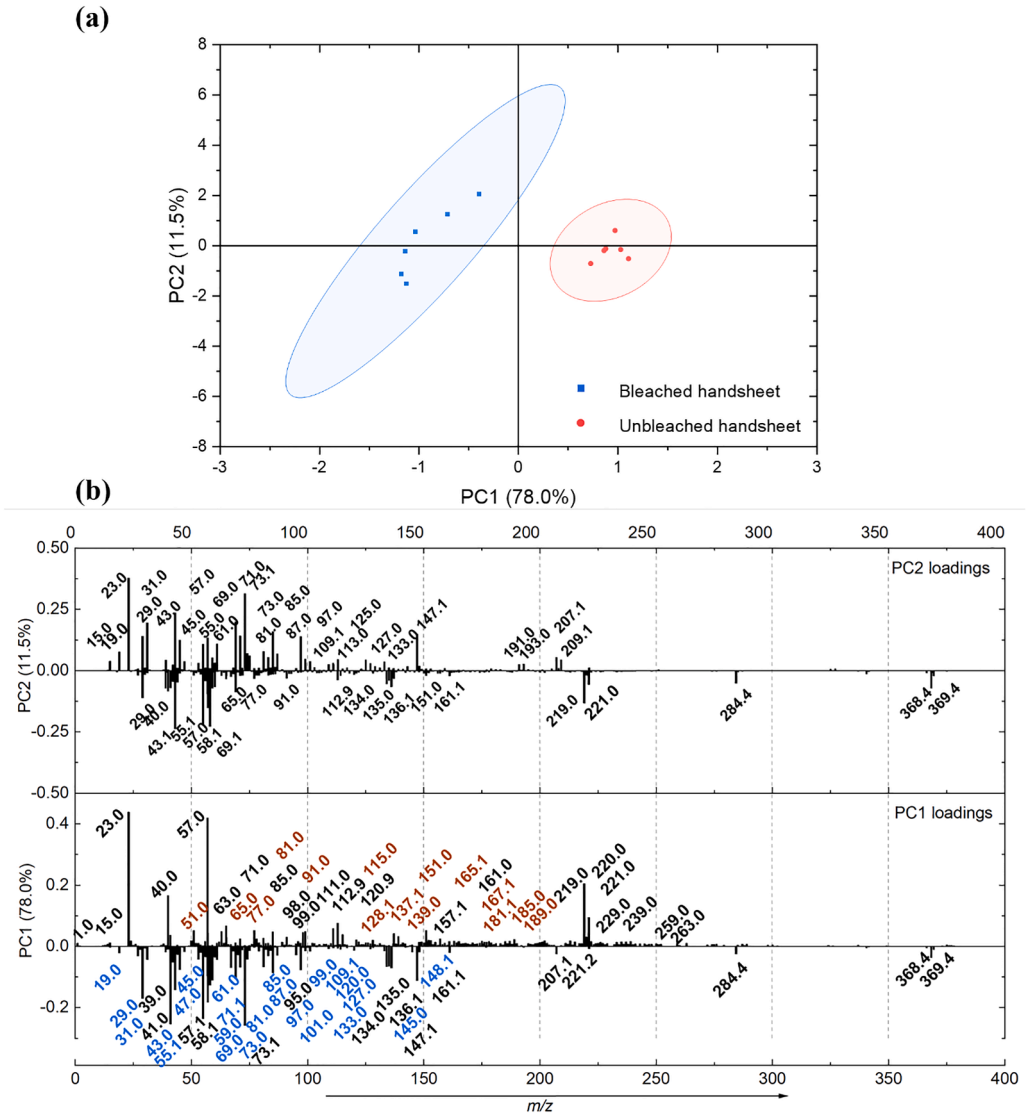


**Fig. 3.** PCA of ToF-SIMS spectra from USK and BSK handsheet surfaces. (a) Score plot with 95% confidence ellipses showing separation between BSK (blue) and USK (red) handsheets. (b) Corresponding PC1 loading plot, displayed up to *m/z* 400 for clarity. Orange labels indicate lignin-associated fragment ions, blue labels indicate polysaccharide-associated fragment ions, and black labels indicate common contaminants or unassigned fragments.

polysaccharides, *m/z* 115⁺ cannot be regarded as a chemically specific marker for either component. It was therefore excluded from the final marker-ion interpretation and considered a non-diagnostic lignocellulosic fragment in the present workflow.

These results underscore the need for contextual marker-ion assignment. Although TIC normalization reduced the differences in the overall secondary-ion yield, several ions appeared on the same side of the PCA loading plot as contaminant-associated signals and were therefore treated as ambiguous or conditionally assigned rather than chemically interpreted. Only ions that were consistent with the reference samples, reproducible across replicates, and supported by the pairwise PCA models were retained in the assigned marker set. This conservative approach reduces the risk of over-interpreting artefactual signals in chemically heterogeneous fiber surfaces and is consistent with recommended practice for ToF-SIMS analysis of lignocellulosic materials.

### 3.2. *Interference from contaminants, adduct formation, and matrix effects*

Given the extreme surface sensitivity of ToF-SIMS, trace contaminants and adduct formation can contribute substantially to the observed spectra and therefore require explicit evaluation. Peaks at *m/z* 73⁺, 147⁺, 207⁺, and 221⁺ were assigned to polydimethylsiloxane (PDMS), a well-known SIMS contaminant arising from common laboratory sources. Because these peaks follow the characteristic 74 Da repeat pattern of PDMS oligomers, they were treated as contamination-related (Bertrand et al., 1996; Goacher et al., 2011; Vickerman, 2013).

Additional signals at *m/z* 134–136⁺ appeared primarily in the BSK handsheet spectra and loaded on the negative PC1 side of Fig. 3b. Their absence or low intensity in the USK samples, together with the pairwise PCA comparisons, suggests that these peaks are not likely to be intrinsic lignocellulosic fragments. In the absence of reference standards or MS/MS confirmation, they were therefore treated as unresolved and excluded from chemically targeted interpretation (Iamazaki et al., 2013; Sjöström, 1999).

The USK handsheet spectra also showed higher intensities of *m/z* 23 ($Na^+$) and *m/z* 40 ($Ca^+$), consistent with the higher sodium and calcium contents measured for the corresponding pulp samples (Table ST3). These signals likely reflect cationic counterions associated with anionic groups at the fiber surface, and possibly retain inorganic species, rather than lignin- or carbohydrate-specific marker ions. Likewise, peaks at *m/*

*z* 63.0⁺, 120.9⁺, and 165.1 were not interpreted as definitive lignin or carbohydrate markers, because ions in this range may overlap with sodium- or phosphate-containing interference species previously reported in lignocellulosic ToF-SIMS datasets (Braham et al., 2015; Kleen, 2005; Koljonen et al., 2004b; Lucia, 2001; Mou et al., 2016). Table 3 summarizes only the final tentative assignments retained after reference-supported screening and conservative interpretation.

In handsheets with chemically heterogeneous fiber-network surfaces, replicate measurements revealed systematic spectral differences, consistent with a delignification-driven shift toward more carbohydrate-associated surface chemistry. However, individual ions can have chemically ambiguous origins.

Six replicate spectra acquired from independent surface locations were evaluated for each sample type using chemometric models (pairwise PCA models), and only ions that consistently contributed to sample separation with statistically significant and chemically interpretable trends were retained as marker ions. The resulting relative abundances of these assigned marker ions are summarized as a violin plot in Fig. 4, where each distribution represents the reproducible contribution of a given ion to the total detected ion population. Under these conditions, the observed intensity trends can be meaningfully interpreted as reflecting surface chemical changes rather than arbitrary spectral fluctuations.

Table 4 summarizes the semi-quantitative surface-chemical differences between USK and BSK handsheet surfaces based on ratios of selected marker ions. The lignin-associated ions at *m/z* 137⁺ and 151⁺ were more intense in the USK handsheets, consistent with the higher residual lignin content before delignification and bleaching. In contrast, several polysaccharide-associated ions showed lower USK-to-BSK ratios, indicating a greater relative contribution of carbohydrate-derived fragments at the BSK fiber surface. The *m/z* 133⁺ ion, characteristic of hexose-derived polysaccharide fragments, showed a lower USK-to-BSK ratio, consistent with increased relative exposure or abundance of hexose-containing polysaccharide material at the bleached fiber surface. Similarly, *m/z* 127⁺ and 145⁺ showed lower ratios, supporting an increased polysaccharide-associated surface character after delignification and bleaching.

These ToF-SIMS trends agree with previous XPS/ESCA and ATR-FTIR studies showing a more oxygen- or carbohydrate-rich surface character after Kraft pulp bleaching (Agarwal et al., 1997; Fardim, Gustafsson et al., 2005; Kleen et al., 2002; Laine et al., 1994, 1996; Mou et al., 2016; Paulsson et al., 2003; Risén et al., 2004). Compared with SEM, AFM, ATR-FTIR, and Raman spectroscopy, ToF-SIMS provides more surface-specific molecular fragment information from the outermost fiber surface, including lignin-, polysaccharide-, extractive- and inorganic-associated ions. However, unlike XPS or vibrational spectroscopy, ToF-SIMS intensities are strongly matrix-dependent and should therefore be interpreted semi-quantitatively rather than as direct surface concentrations.

### 3.3. 2D ToF-SIMS imaging of surface marker ions

Fig. 5 presents representative 2D ToF-SIMS ion images of assigned lignin- and polysaccharide-associated markers found on USK and BSK handsheets. These images are presented as qualitative examples to complement the spectroscopic and chemometric analyses. Fig. 5a and d show the total-ion images of the USK and BSK handsheets, respectively; Fig. 5b, c, e, and f show lignin-associated ions; and Fig. 5g–l show polysaccharide-associated ions. The molecular structures assigned to the selected marker ions are shown below the corresponding 2D ion images.

The *m/z* 145⁺ ion appeared less distinct in the USK than in the BSK handsheet, whereas the *m/z* 127⁺ ion remained visible in both. This difference is consistent with stronger matrix suppression of higher-mass, oxygen-rich carbohydrate fragments at lignin-richer surfaces, as reported previously for lignocellulosic ToF-SIMS analyses (Goacher et al., 2011). The increased intensity of *m/z* 133⁺ after bleaching further

**Table 3**
Tentative peak assignment for the positive secondary ions in the ToF-SIMS spectrum, PS = polysaccharides, L = lignin.

| *m/z* (dev. in ppm) | Assignment | Classification by PCA | *m/z* (dev. in ppm) | Assignment | Classification by PCA | *m/z* (dev. in ppm) | Assignment | Classification by PCA |
|---|---|---|---|---|---|---|---|---|
| 19.0⁺(11.9) | $H_3O^+$ | - | 87.0 (−13.8) | $C_4H_7O_2^+$ | PS | 51.0⁺ (−20.7) | $C_4H_3^+$ | L |
| 29.0⁺ (22.7) | $C_2H_5^+$ | PS | 97.0⁺ (−3.8) | $C_5H_5O_2^+$ | PS | 55⁺ (−18.3) | $C_4H_7^+$ | L |
| 31.0⁺ (23.5) | $CH_3O^+$ | PS | 99.0⁺ (−19.4) | $C_5H_7O_2^+$ | PS | 65.0⁺ (−4.2) | $C_5H_5^+$ | L |
| 43.0⁺ (−15.6) | $C_3H_7^+$ | PS | 101.0⁺ (−19.5) | $C_4H_5O_3^+$ | PS | 77.0⁺ (−16.6) | $C_6H_5^+$ | L |
| 45.0⁺ (−3.8) | $C_2H_5O^+$ | PS | 109.0⁺ (−26.5) | $C_6H_5O_2^+$ | PS | 81.0⁺ (23.1) | $C_6H_9^+$ | L |
| 47.0⁺ (−38.6) | $CH_3O_2^+$ | PS | 113.0⁺ (36.7) | $C_5H_5O_3^+$ | PS | 91.0⁺ (−2.8) | $C_7H_7^+$ | L |
| 55.1⁺ (−8.9) | $C_3H_3O^+$ | PS | 115.0⁺ (38.2) | $C_5H_7O_3^+$ | PS | 115.0⁺ (−17.0) | $C_9H_7^+$ | L |
| 57.0⁺ (20.3) | $C_3H_5O^+$ | PS | 120.0⁺ (9.8) | $C_8H_8O^+$ | PS | 128.1⁺ (60.5) | $C_6H_8O_3^+$ | L |
| 59.1⁺ (−15.6) | $C_2H_3O_2^+$ | PS | 127.0⁺ (−13.7) | $C_6H_7O_3^+$ | PS | 137.0⁺ (8.0) | $C_8H_9O_2^+$ | L |
| 61.0⁺ (−21.9) | $C_2H_5O_2^+$ | PS | 133.0⁺ (12.2) | $C_5H_9O_4^+$ | PS | 139.0⁺ (79.2) | $C_7H_7O_3^+$ | L |
| 69.0⁺ (−10.7) | $C_4H_5O^+$ | PS | 145.0⁺ (8.2) | $C_6H_9O_4^+$ | PS | 151.0⁺ (1.4) | $C_8H_7O_3^+$ | L |
| 71.0⁺ (−18.4) | $C_3H_3O_2^+$ | PS | 148.1⁺ (−16.9) | $C_6H_{12}O_4^+$ | PS | 165.1⁺ (−34.9) | $C_9H_9O_3^+$ | L |
| 73.0⁺ (−18.3) | $C_3H_5O_2^+$ | PS | 161⁺ (22.4) | $C_6H_9O_5^+$ | PS | 167.1⁺ (−5.4) | $C_9H_{11}O_3^+$ | L |
| 81.0⁺ (−15.3) | $C_5H_5O^+$ | PS | 163⁺ (−18.7) | $C_6H_{11}O_5^+$ | PS | 181.1⁺ (7.6) | $C_9H_9O_4^+$ | L |
| 85.0⁺ (20.3) | $C_4H_5O_2^+$ | PS | 29.0⁺ (−1.2) | $CHO^+$ | L | 185.0⁺ (74.6) | $C_8H_9O_5^+$ | L |
| 87.0⁺ (−2.8) | $C_4H_7O_2^+$ | PS | 43.1⁺ (−12.6) | $C_3H_7^+$ | L | 189.0⁺ (−18.1) | $C_{11}H_9O_3^+$ | L |

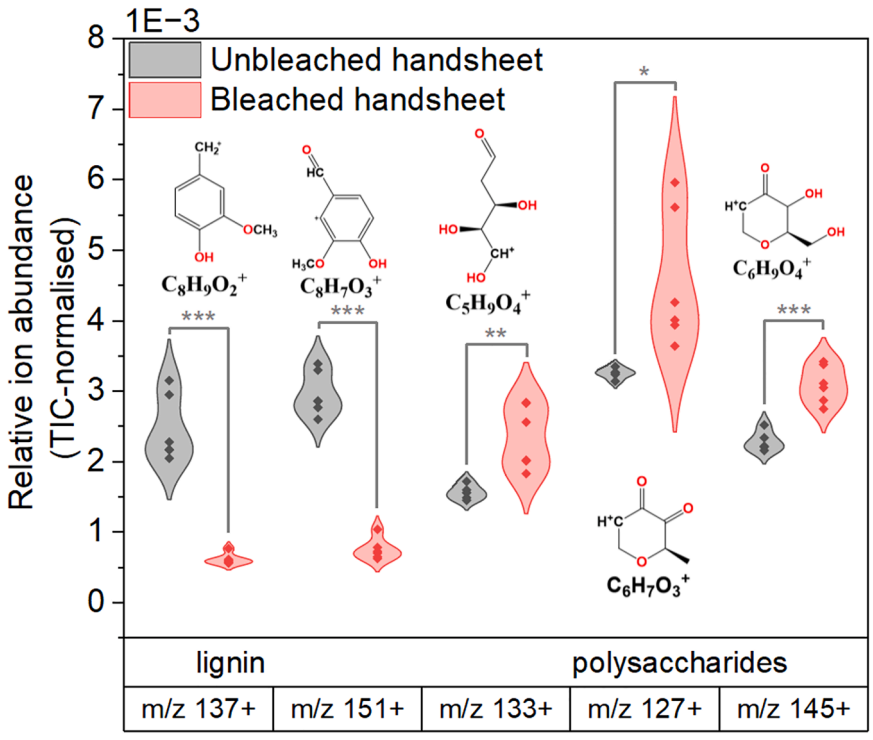


**Fig. 4.** Violin-box plot of the fragment ion abundance profiles in USK and BSK handsheets. (Statistical significance was assessed using Welch's two-sample *t*-test from six measurements per sample class. Asterisks indicate significance levels: *** $p < 0.001$, ** $p < 0.01$, * $p < 0.05$).

**Table 4**
Relative intensity ratios of assigned marker ions for USK versus BSK handsheets.

| Peak *(m/z)* | Assignment | Ratio $= \frac{I_{USK\ handsheet}}{I_{BSK\ handsheet}}$ |
|---|---|---|
| $137^+$ | Lignin | 4.03 (1.03) |
| $151^+$ | Lignin | 4.01 (0.89) |
| $115^+$(L/PS isobar) | Lignin/ Polysaccharide | 1.37 (0.09) |
| $133^+$ | Hemicellulose | 0.69 (0.12) |
| $127^+$ | Cellulose | 0.76 (0.16) |
| $145^+$ | Cellulose | 0.75 (0.08) |

Values in brackets are the standard error from six measurements.

suggests a higher relative contribution from polysaccharide-associated fragments at the BSK handsheet surface. The representative ion images are consistent with the spectroscopic and chemometric analyses, indicating that bleaching decreases the relative surface contribution of lignin-associated chemistry while increasing polysaccharide-associated surface character.

## 4. Conclusion

A semi-quantitative ToF-SIMS workflow was developed for chemically complex softwood Kraft handsheet surfaces. By combining mechanically compacted reference samples with total-ion-count normalization, pairwise PCA, and conservative marker-ion screening, the workflow enabled reproducible interpretation of cellulose-, hemicellulose-, and lignin-associated ion patterns despite surface heterogeneity, matrix effects, and isobaric overlap.

When applied to unbleached and bleached fiber surfaces within handsheets, the workflow confirmed the expected bleaching-related decrease in the relative contribution of lignin-associated surface chemistry, together with an increase in polysaccharide-associated surface chemistry. Unbleached handsheets showed stronger contributions from guaiacyl lignin-associated ions, particularly *m/z* $137^+$ and $151^+$, whereas bleached handsheets showed enhanced contributions from polysaccharide-associated ions, including *m/z* $127^+$, $133^+$, and $145^+$. The 2D ion images supported the same directional trend by showing stronger and more spatially distributed polysaccharide-associated signals after bleaching.

The main value of the present ToF-SIMS workflow lies in extending surface analysis beyond average compositional trends by providing fragment-level and spatially resolved chemical information at chemically heterogeneous fiber surfaces. Its contribution is therefore not the assignment of every ion as uniquely diagnostic, but the establishment of a reference-guided and chemically conservative strategy for interpreting complex ToF-SIMS spectra from fiber materials. The disadvantage of ToF-SIMS is that its spectra are more complex and less straightforward to quantify than ESCA/XPS. Matrix effects, isobaric overlap, adduct formation, and contamination can complicate direct interpretation, so chemically meaningful conclusions usually require reference samples, replicate measurements, and conservative assignment criteria. Its advantage is that it can resolve which ion families contribute to a surface-chemical contrast and where those signals are distributed across the surface, rather than only indicating an average surface-composition trend. In the present case, ToF-SIMS showed not only that bleaching changes the outermost surface chemistry of softwood Kraft handsheets, but also which lignin-associated and polysaccharide-associated fragment patterns drive that difference and how these signals are distributed across heterogeneous fiber-network surfaces. The present workflow also provides a foundation for future quantitative spatial analyses, including objective evaluation of marker-ion distributions, co-localization, and spatial heterogeneity across lignocellulosic fibre surfaces. In this form, the workflow provides a practical basis for studying paper surfaces, fiber modification, coating interactions, and other carbohydrate-polymer interfaces in lignocellulosic materials.

### Declaration of generative AI and AI-assisted technologies in the writing process

During the preparation of this work, the authors used Microsoft

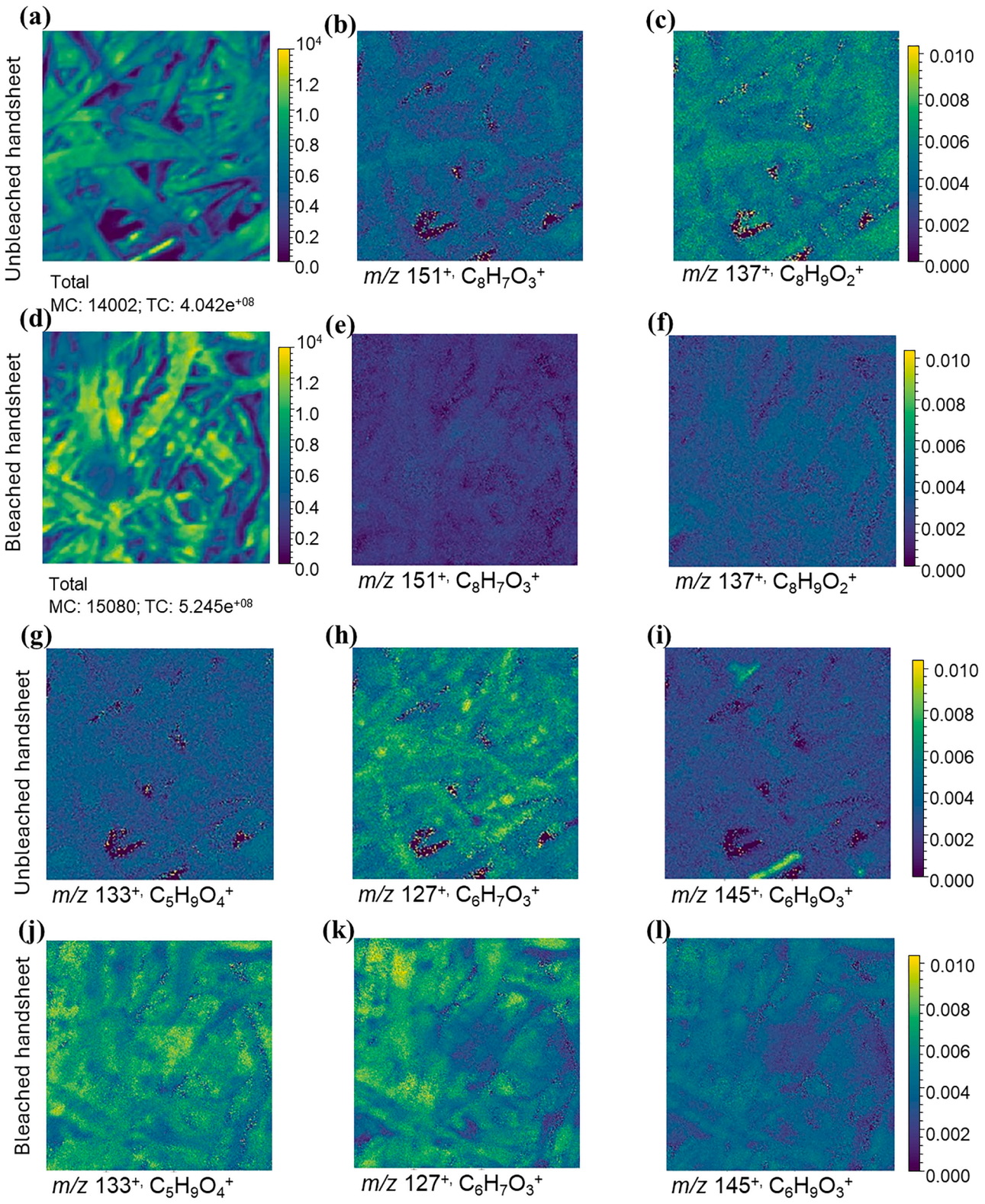


**Fig. 5.** Representative ToF-SIMS ion images of USK and BSK handsheet surfaces illustrating the spatial distributions of selected lignin- and polysaccharide-associated marker ions. Panels (a and d) show total-ion images; panels (b, c, e, f) show lignin-associated ions; and panels (g–l) show polysaccharide-associated ions. Field of view: 500 × 500 μm$^2$; 25 scans for acquisition; MC = Maximum counts in a single pixel; TC = Total counts summed over the image.

Copilot to improve language, clarity and readability of the manuscript text. After using this tool, the authors reviewed and edited the content as needed and take full responsibility for the final version of the manuscript.

**Funding**

This project was financed by the Bo Rydins Stiftelse för vetenskaplig forskning, and FibRe – Design for circularity – Lignocellulose-based thermoplastics, a VINNOVA competence centre (2019-00047).

## CRediT authorship contribution statement

**Nivedhitha Venkatraman:** Writing – review & editing, Writing – original draft, Visualization, Validation, Software, Methodology, Investigation, Formal analysis, Data curation, Conceptualization. **Per A. Larsson:** Writing – review & editing, Writing – original draft, Supervision, Conceptualization. **Anette Larsson:** Writing – review & editing, Writing – original draft, Supervision, Resources, Project administration, Investigation, Funding acquisition, Conceptualization. **Per Malmberg:** Writing – review & editing, Writing – original draft, Validation, Supervision, Software, Resources, Project administration, Methodology, Investigation, Funding acquisition, Formal analysis, Data curation, Conceptualization.

## Declaration of competing interest

The authors declare that they have no known competing financial interests or personal relationships that could have appeared to influence the work reported in this paper.

## Acknowledgements

We acknowledge support from the Bo Rydin Foundation and the FibRe Centre for Lignocellulose-based Thermoplastics VINNOVA competence centre (2019-00047).

The ToF-SIMS investigations were carried out using the Chemical Imaging Infrastructure (CII) Research and Technology Platform, which was funded by the Knut and Alice Wallenberg Foundation via the Wallenberg Initiative Materials Science for Sustainability (WISE).

This project was performed partly at Chalmers Materials Analysis Laboratory (CMAL). We also thank Åke Henrik-Klemens for providing samples, and Anders Brolin (Stora Enso AB) for scientific feedback on the manuscript.

## Supplementary materials

Supplementary material associated with this article can be found, in the online version, at doi:10.1016/j.carpta.2026.101209.

## Data availability

Data will be made available on request.

## References

Agarwal, U., & Ralph, S. (1997). FT-raman spectroscopy of wood: Identifying contributions of lignin and carbohydrate polymers in the spectrum of black spruce (Picea Mariana). *Applied Spectroscopy, 51*, 1648–1655.

Åvitsland, G. A., & Wågberg, L. (2005). Flow resistance of wet and dry sheets used for preparation of liquid packaging board. *Nordic Pulp and Paper Research Journal, 20*, 345–353.

Bertrand, P., & Lu-Tao, W. (1996). Time-of-flight secondary ion mass spectrometry (ToF-SIMS). In D. Benoit, J.-F. Bresse, L. Van't dack, H. Werner, & J. Wernisch (Eds.), *Microbeam and nanobeam analysis* (pp. 167–182). Vienna: Springer Vienna.

Braham, E. J., & Goacher, R. E. (2015). Identifying and minimizing buffer interferences in ToF-SIMS analyses of lignocellulose. *Surface and Interface Analysis, 47*(1), 120–126.

Eliasson, A., Hedenqvist, M., Brolin, A., Wågberg, L., & Malmström, E. (2023). Highly ductile cellulose-rich papers obtained by ultrasonication-assisted incorporation of low molecular weight plasticizers. *ACS Sustainable Chemistry & Engineering, 11*(24), 8836–8846.

Fardim, P., & Durán, N. (2003). Modification of fibre surfaces during pulping and refining as analysed by SEM, XPS and ToF-SIMS. *Colloids and Surfaces A: Physicochemical and Engineering Aspects, 223*(1), 263–276.

Fardim, P., Gustafsson, J., von Schoultz, S., Peltonen, J., & Holmbom, B. (2005). Extractives on fiber surfaces investigated by XPS, ToF-SIMS and AFM. *Colloids and Surfaces A: Physicochemical and Engineering Aspects, 255*(1), 91–103.

Fardim, P., & Holmbom, B. (2005). ToF-SIMS imaging: A valuable chemical microscopy technique for paper and paper coatings. *Applied Surface Science, 249*(1), 393–407.

Forsström, J., Torgnysdotter, A., & Wågberg, L. (2005). Influence of fibre/fibre joint strength and fibre flexibility on the strength of papers from unbleached kraft fibres. *Nordic Pulp and Paper Research Journal, 20*, 186–191.

Goacher, R. E., Jeremic, D., & Master, E. R. (2011). Expanding the library of secondary ions that distinguish lignin and polysaccharides in time-of-flight secondary ion mass spectrometry analysis of wood. *Analytical Chemistry, 83*(3), 804–812.

Goacher, R. E., & Michienzi, C. L. (2018). How does soaking wood in various pH buffers impact ToF-SIMS spectra? *Surface and Interface Analysis, 50*(2), 163–170.

Goacher, R. E., Tsai, A. Y.-L., & Master, E. R. (2013). Towards practical time-of-flight secondary ion mass spectrometry lignocellulolytic enzyme assays. *Biotechnology for Biofuels, 6*(1), 132.

Guerra, A., Gaspar, A. R., Contreras, S., Lucia, L. A., Crestini, C., & Argyropoulos, D. S. (2007). On the propensity of lignin to associate: A size exclusion chromatography study with lignin derivatives isolated from different plant species. *Phytochemistry, 68*(20), 2570–2583.

Henrik-Klemens, Å., Caputo, F., Ghaffari, R., Westman, G., Edlund, U., Olsson, L., & Larsson, A. (2024). The glass transition temperature of isolated native, residual, and technical lignin. *Holzforschung, 78*(4), 216–230.

Henriksson, G., Germgård, U., & Lindström, M. E. (2024). A review on chemical mechanisms of kraft pulping. *Nordic Pulp & Paper Research Journal, 39*(3), 297–311.

Iamazaki, E. T., Orblin, E., & Fardim, P. (2013). Topochemical activation of pulp fibres. *Cellulose (London, England), 20*(5), 2615–2624.

Jääskeläinen, A. S., Sun, Y., Argyropoulos, D. S., Tamminen, T., & Hortling, B. (2003). *The effect of isolation method on the chemical structure of residual lignin, 37* pp. 91–102). Wood Science and Technology.

Jin, H., Kose, R., Akada, N., & Okayama, T. (2022). Relationship between wettability of pulp fibers and tensile strength of paper during recycling. *Scientific Reports, 12*(1).

Kesari, K. K., Leppänen, M., Ceccherini, S., Seitsonen, J., Väisänen, S., Altgen, M., … Vuorinen, T. (2020). Chemical characterization and ultrastructure study of pulp fibers. *Materials Today Chemistry, 17*, Article 100324.

Kleen, M. (2005). Surface lignin and extractives on hardwood RDH kraft pulp chemically characterized by ToF-SIMS. *Holzforschung, 59*(5), 481–487.

Kleen, M., Sjöberg, J., Dahlman, O., Johansson, L.-S., Koljonen, K., & Stenius, P. (2002). The effect of ECF and TCF bleaching on the chemical composition of soda-anthraquinone and kraft pulp surfaces. *Nordic Pulp and Paper Research Journal, 17*(3), 357–363.

Koljonen, K. (2004). *Effect of surface properties of fibres on some paper properties of mechanical and chemical pulp*. Helsinki University of Technology Department of Forest Products Technology Laboratory of Forest Products Chemistry. *951-22-7267-9* (Vol. Degree of Doctor of Science in Technology).

Koljonen, K., Österberg, M., Kleen, M., Fuhrmann, A., & Stenius, P. (2004a). Precipitation of lignin and extractives on kraft pulp: Effect on surface chemistry, surface morphology and paper strength. *Cellulose (London, England), 11*(2), 209–224.

Koljonen, K., Österberg, M., Kleen, M., Fuhrmann, A., & Stenius, P. (2004b). Precipitation of lignin and extractives on kraft pulp: Effect on surface chemistry, surface morphology and paper strength. *Cellulose (London, England), 11*, 209–224.

Laine, J., Stenius, P., Carlsson, G., & Ström, G. (1994). Surface characterization of unbleached kraft pulps by means of ESCA. *Cellulose (London, England), 1*(2), 145–160.

Laine, J., Stenius, P., Carlsson, G., & Ström, G. (1996). The effect of ECF and TCF bleaching on the surface chemical composition of kraft pulp as determined by ESCA. *Nordic Pulp and Paper Research Journal, 11*, 201–210.

Lee, J. L. S., Gilmore, I. S., & Seah, M. P. (2008). Quantification and methodology issues in multivariate analysis of ToF-SIMS data for mixed organic systems. *Surface and Interface Analysis, 40*(1), 1–14.

Letourneau, D. R., & Volmer, D. A. (2023). Mass spectrometry-based methods for the advanced characterization and structural analysis of lignin: A review. *Mass Spectrometry Reviews, 42*(1), 144–188.

Lucia, L., & Mancosky, D. G. (2001). Use of TOF-SIMS for the analysis of surface metals in H2O2-bleached lignocellulosic fibers. *Pure and Applied Chemistry, 73*(12), 2047–2058.

Morreel, K., Kim, H., Lu, F., Dima, O., Akiyama, T., Vanholme, R., …, & Boerjan, W. (2010). Mass spectrometry-based fragmentation as an identification tool in lignomics. *Analytical Chemistry, 82*(19), 8095–8105.

Mou, H. Y., Wu, S., & Fardim, P. (2016). Applications of ToF-SIMS in surface chemistry analysis of lignocellulosic biomass: A review. *BioResources, 11*, 5581–5599.

Oinonen, P. (2014). A biomimicking approach for hemicellulose processing. TRITA-CHE-Report (p. 50). Stockholm: KTH Royal Institute of Technology.

Paulsson, M., & Heijnesson Hultén, A. (2003). Surface characterization of unbleached and oxygen delignified kraft pulp fibers. *Journal of Wood Chemistry and Technology, 23*(1), 31–46.

Reale, S., Tullio, A., Spreti, N., & De Angelis, F. (2004). Mass spectrometry in the biosynthetic and structural investigation of lignins. *Mass Spectrometry Reviews, 23*, 87–126.

Risén, J., Hultén, A. H., & Paulsson, M. (2004). Surface characterization of softwood and hardwood kraft pulp fibers from different stages in a bleaching sequence. *Journal of Wood Chemistry and Technology, 24*, 307–321.

Saito, K., Kato, T., Takamori, H., Kishimoto, T., Yamamoto, A., & Fukushima, K. (2006). A new analysis of the depolymerized fragments of lignin polymer in the plant cell walls using ToF-SIMS. *Applied Surface Science, 252*(19), 6734–6737.

Saito, K., Kato, T., Tsuji, Y., & Fukushima, K. (2005). Identifying the characteristic secondary ions of lignin polymer using ToF−SIMS. *Biomacromolecules, 6*(2), 678–683.

Sjöström, E. (1999). *Analytical methods in wood chemistry, pulping, and papermaking* (1st ed.). Berlin, Heidelberg: Springer.

Tokareva, E. N., Pranovich, A. V., & Holmbom, B. R. (2011). Characteristic fragment ions from lignin and polysaccharides in ToF–SIMS. *Wood Science and Technology, 45*(4), 767–785.

Tolbert, A., & Ragauskas, A. J. (2017). Advances in understanding the surface chemistry of lignocellulosic biomass via time-of-flight secondary ion mass spectrometry. *Energy Science & Engineering, 5*(1), 5–20.
Vickerman, J. C. B., & David. (2013). *ToF-SIMS: Materials analysis by mass spectrometry*. Chichester, UK: IM Publications.
Wålinder, M. E. P., & Ström, G. (2001). Measurement of wood wettability by the Wilhelmy method. Part 2. Determination of apparent contact angles. *Holzforschung, 55*(1), 33–41.
Watts, J., & Goacher, R. (2022). A guide for the meaningful surface analysis of wood by XPS and ToF-SIMS. *Surface and Interface Analysis, 54*(4), 389–404.
Zhou, C., Li, Q., Chiang, V. L., Lucia, L. A., & Griffis, D. P. (2011). Chemical and spatial differentiation of Syringyl and Guaiacyl lignins in Poplar wood via time-of-flight secondary ion mass spectrometry. *Analytical Chemistry, 83*(18), 7020–7026.